Electronic Supplementary Information

Benzimidazole–acid hydrazide Schiff–Mannich combo ligands enable nano–molar detection of Zn^{2+} via fluorescence turn–on mode from semi–aqueous medium, HuH–7 cells, and plants

Riya Bag,[a] Yeasin Sikdar,[a§*] Sutapa Sahu,[a] Md Majharul Islam,[b] Sukhendu Mandal,[b] Sanchita Goswami [a*]

[a]*Department of Chemistry, University of Calcutta, 92, A.P.C. Road, Kolkata 700009, India.*

E–mail: sgchem@caluniv.ac.in (S.G.), y.sikdar@gmail.com (Y.S.)

[b]*Department of Microbiology, University of Calcutta, 35, Ballygunge Circular Road, Kolkata, India.*

[§]*Present address: Department of Chemistry, The Bhawanipur Education Society College, 5, Lala Lajpat Rai Sarani, Kolkata 700020, India.*

Contents

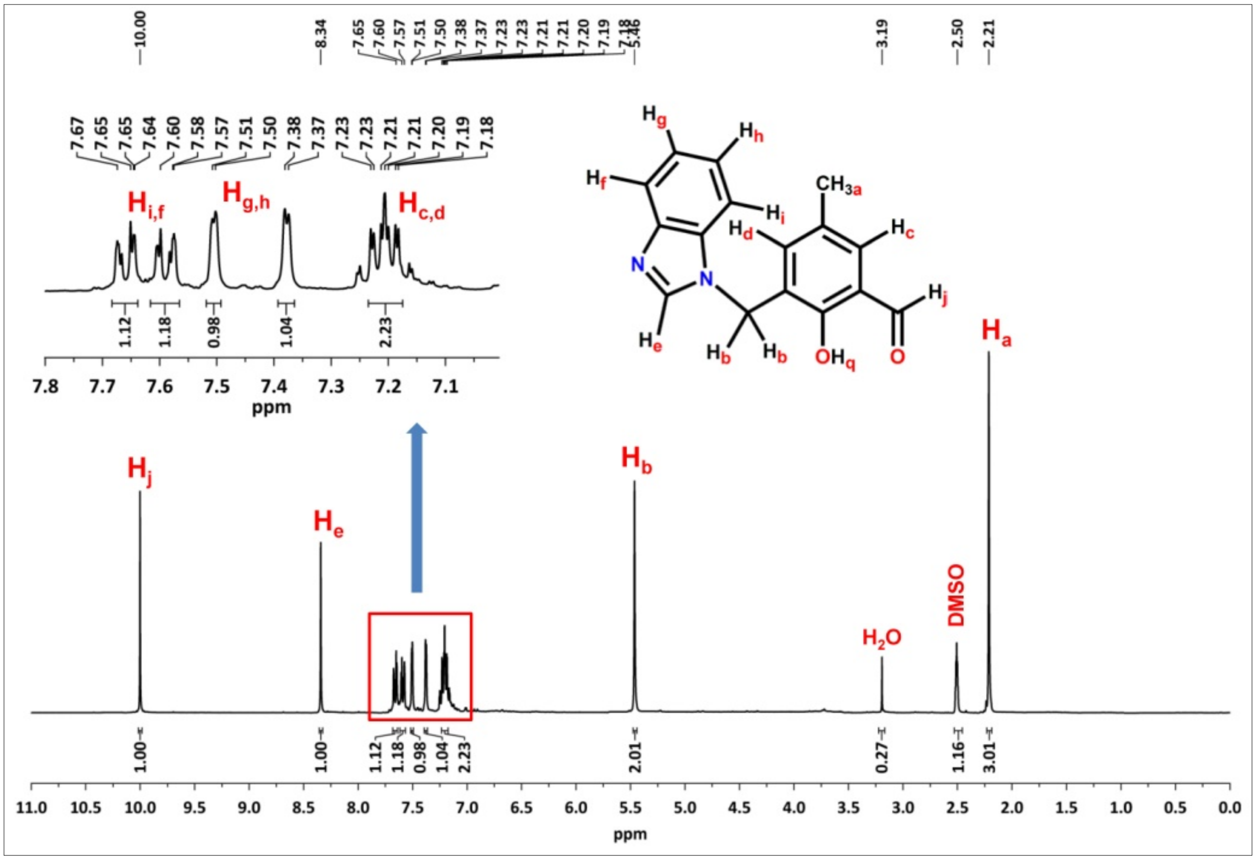

Fig. S1 ^{1}H NMR spectra of HBA in DMSO–d_6.

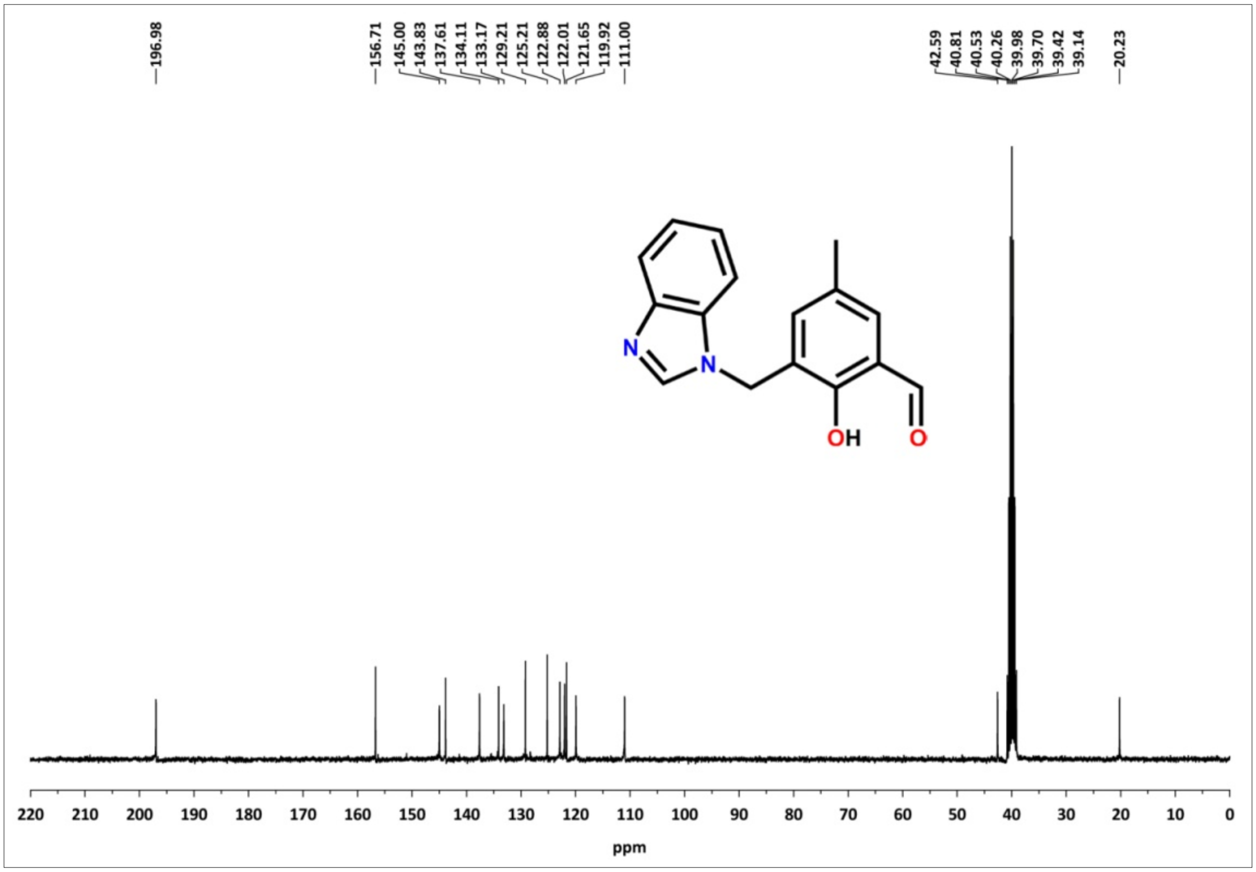

Fig. S2 ^{13}C NMR spectra of HBA in DMSO–d_6.

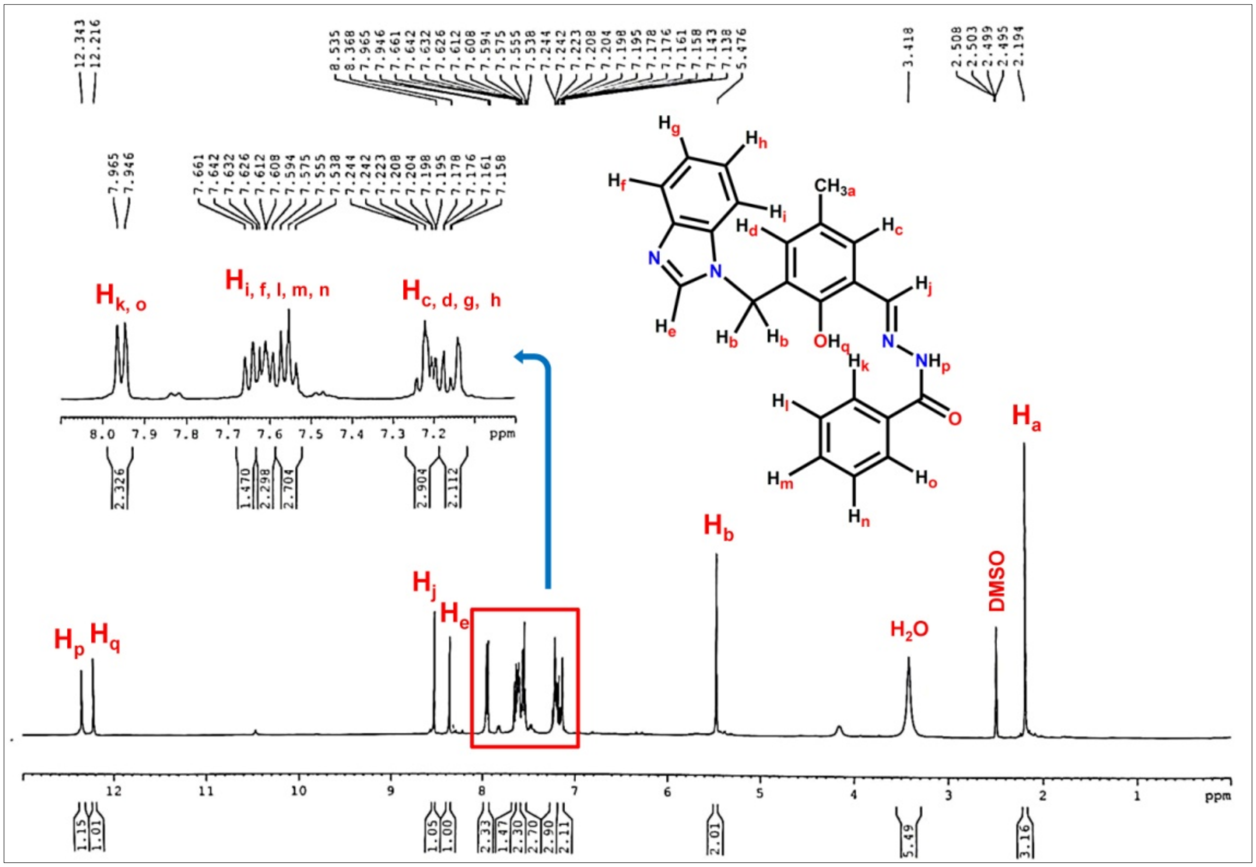

Fig. S3 ^{1}H NMR spectrum of $\mathbf{H_2BBH}$ in DMSO–d_6.

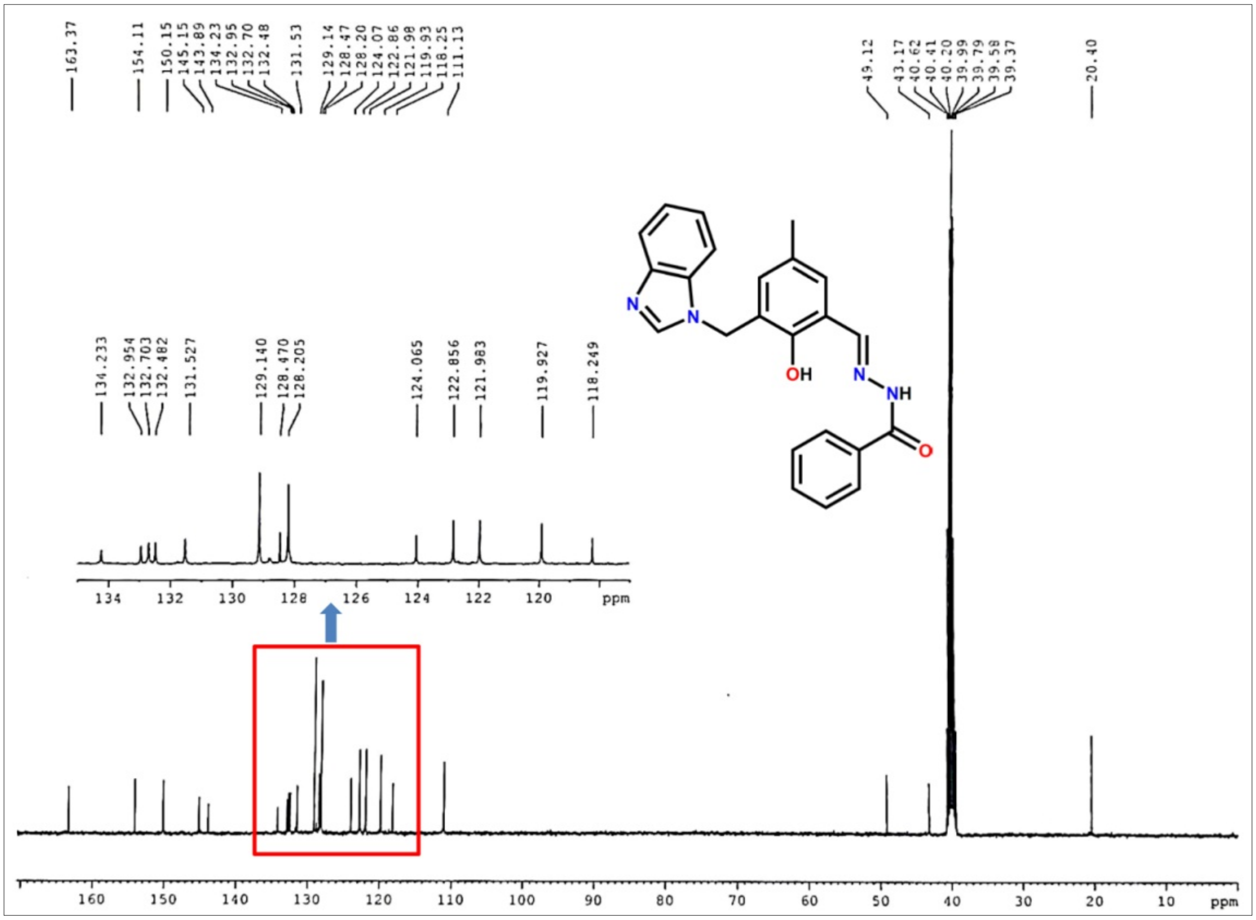

Fig. S4 ^{13}C NMR spectrum of **H$_2$BBH** in DMSO–d_6.

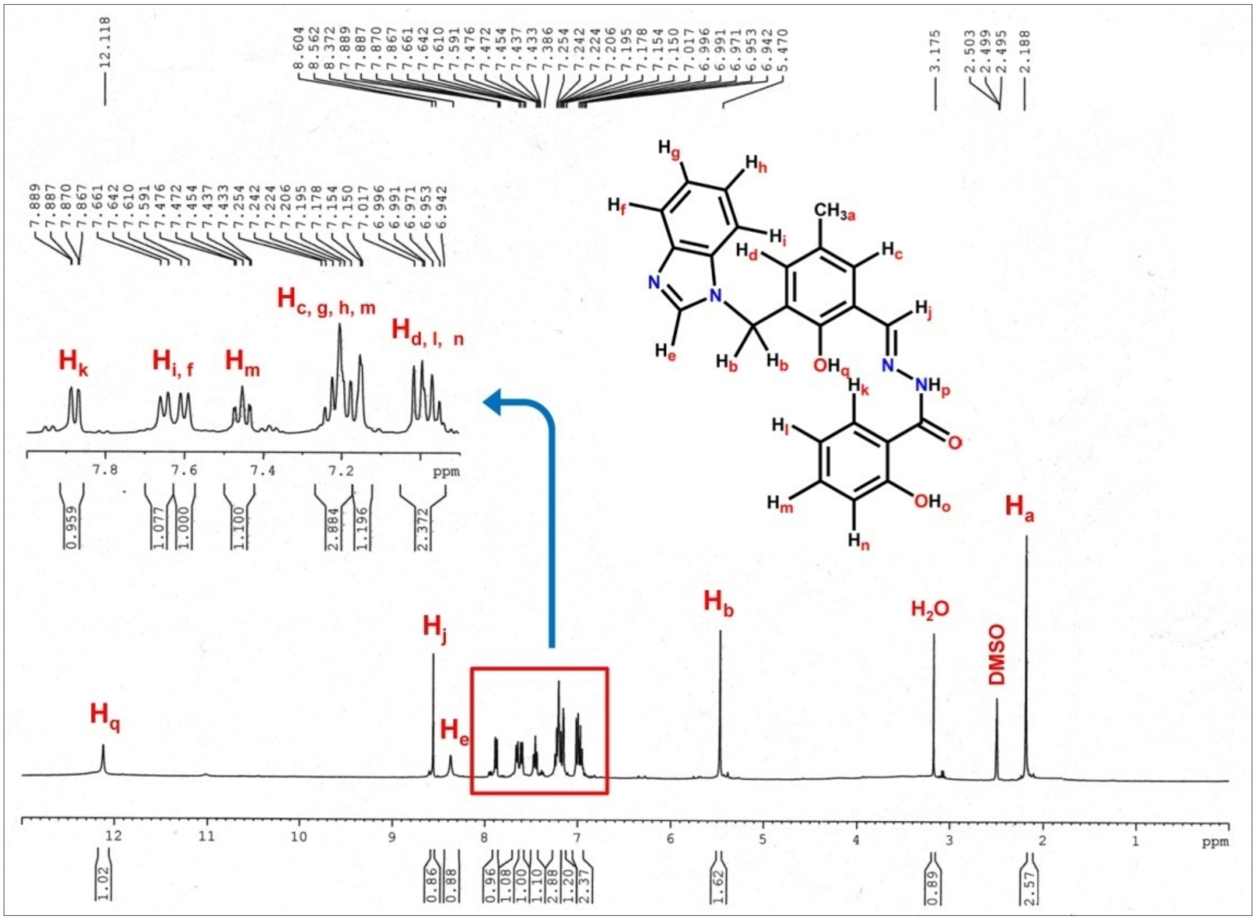

Fig. S5 ^{1}H NMR spectrum of $\mathbf{H_3BSH}$ in DMSO–d_6.

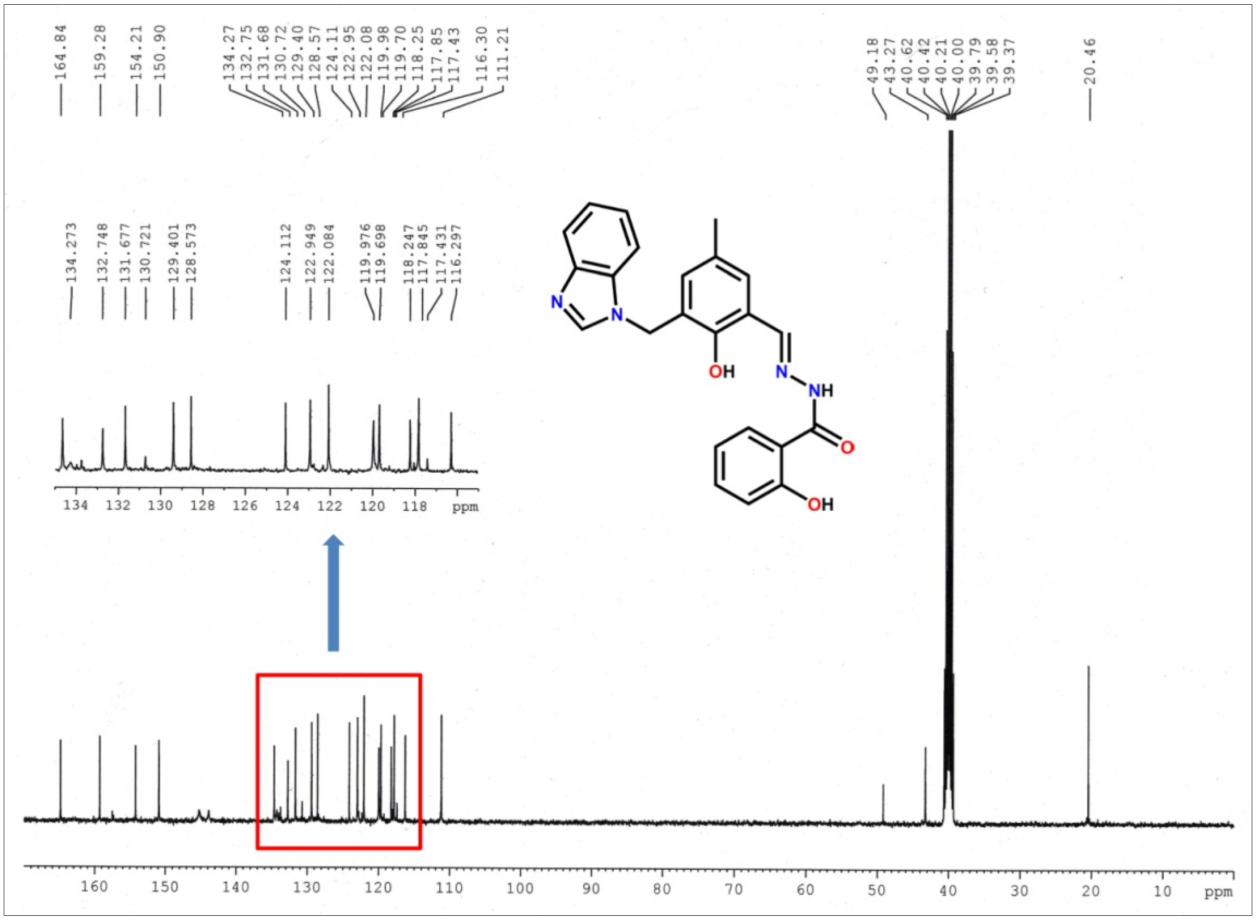

Fig. S6 ^{13}C NMR spectrum of **H_3BSH** in DMSO–d_6.

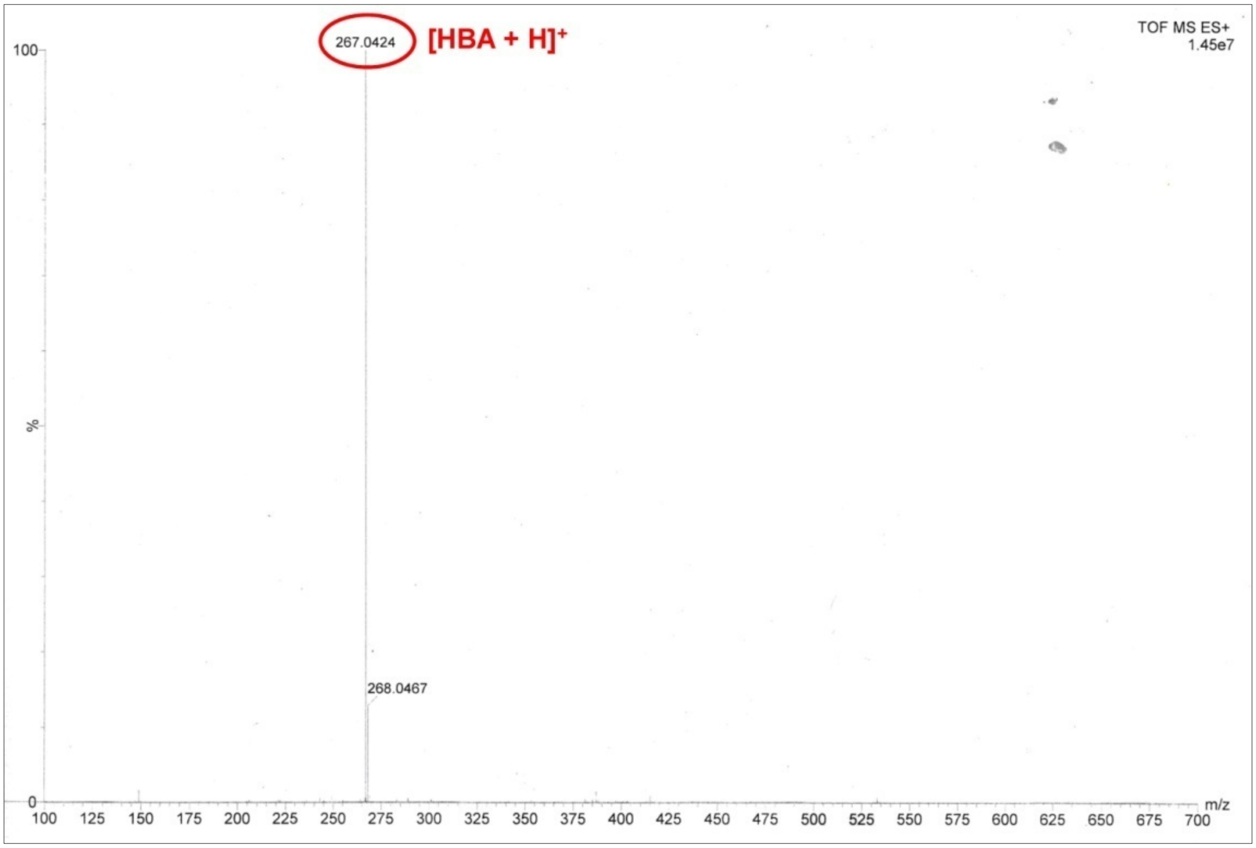

Fig. S7 ESI–MS spectra of HBA.

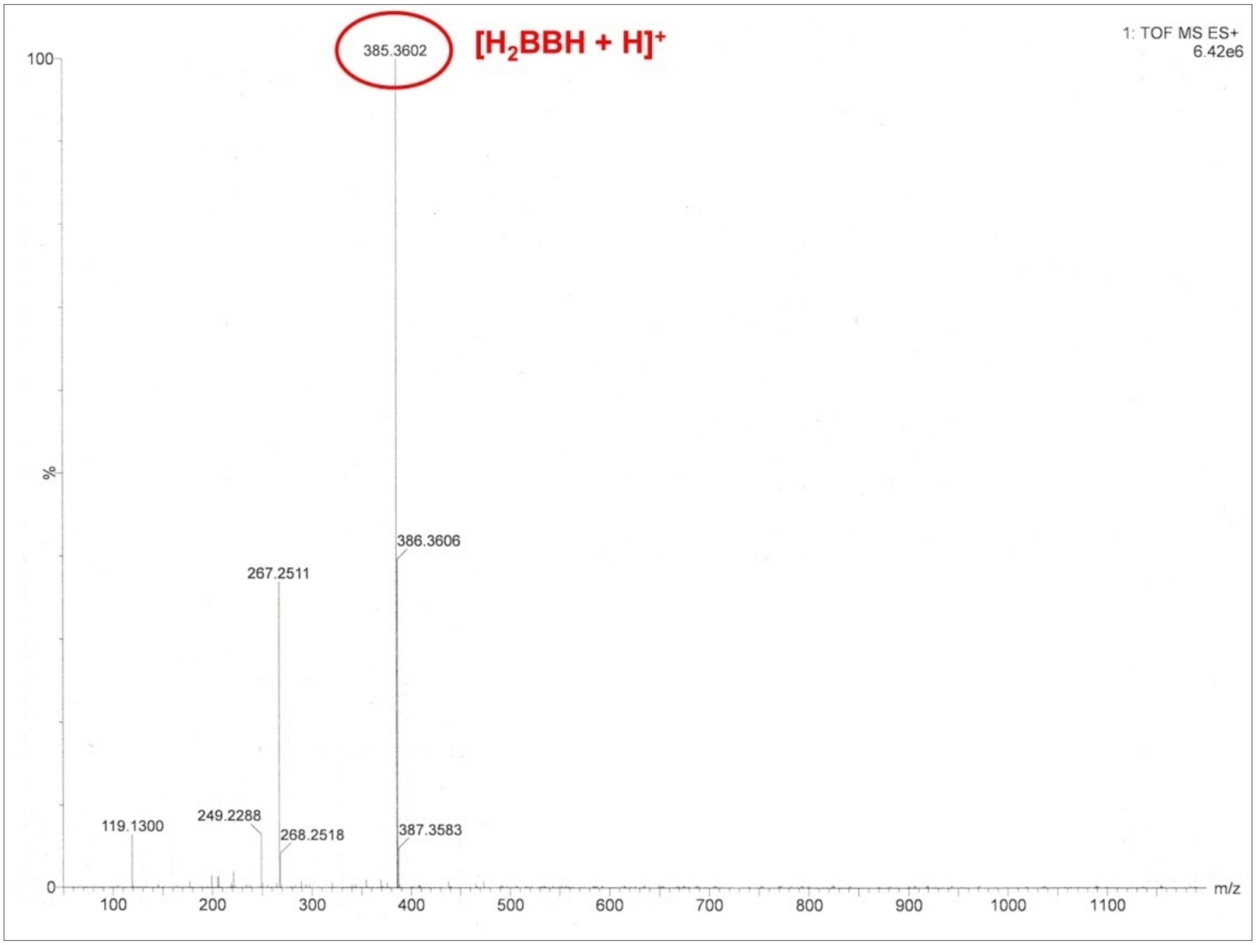

Fig. S8 ESI–MS spectrum of **H_2BBH**.

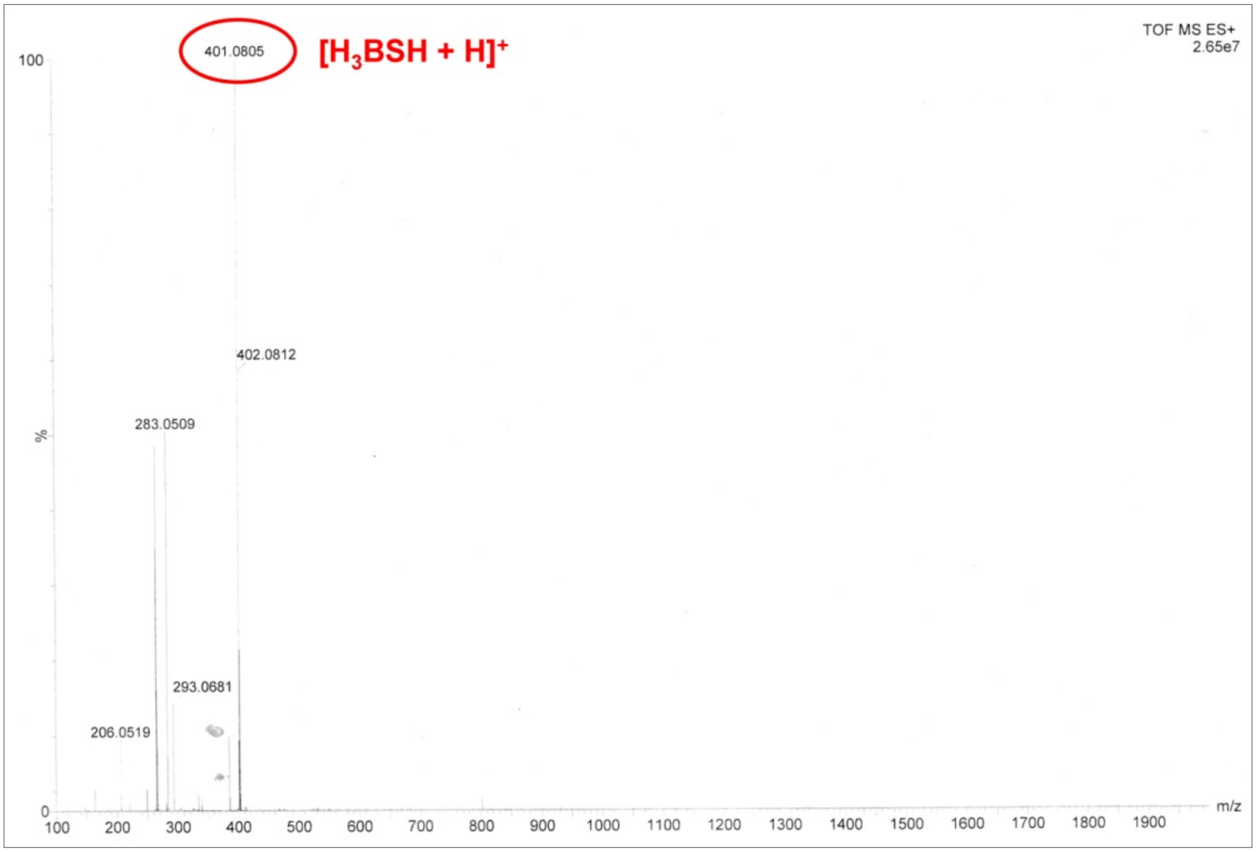

Fig. S9 ESI–MS spectrum of $\mathbf{H_3BSH}$.

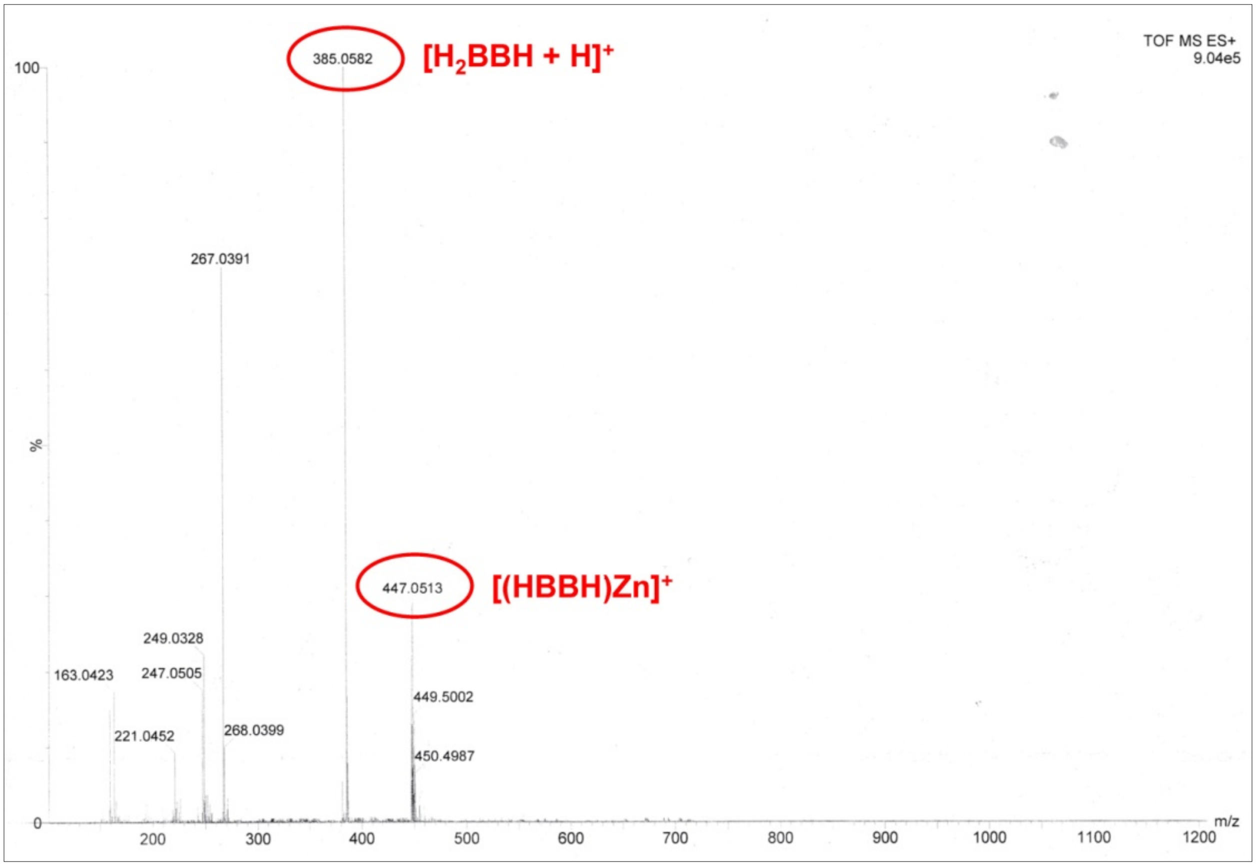

Fig. S10 ESI–MS spectrum of $[(HBBH)_2Zn]$ complex.

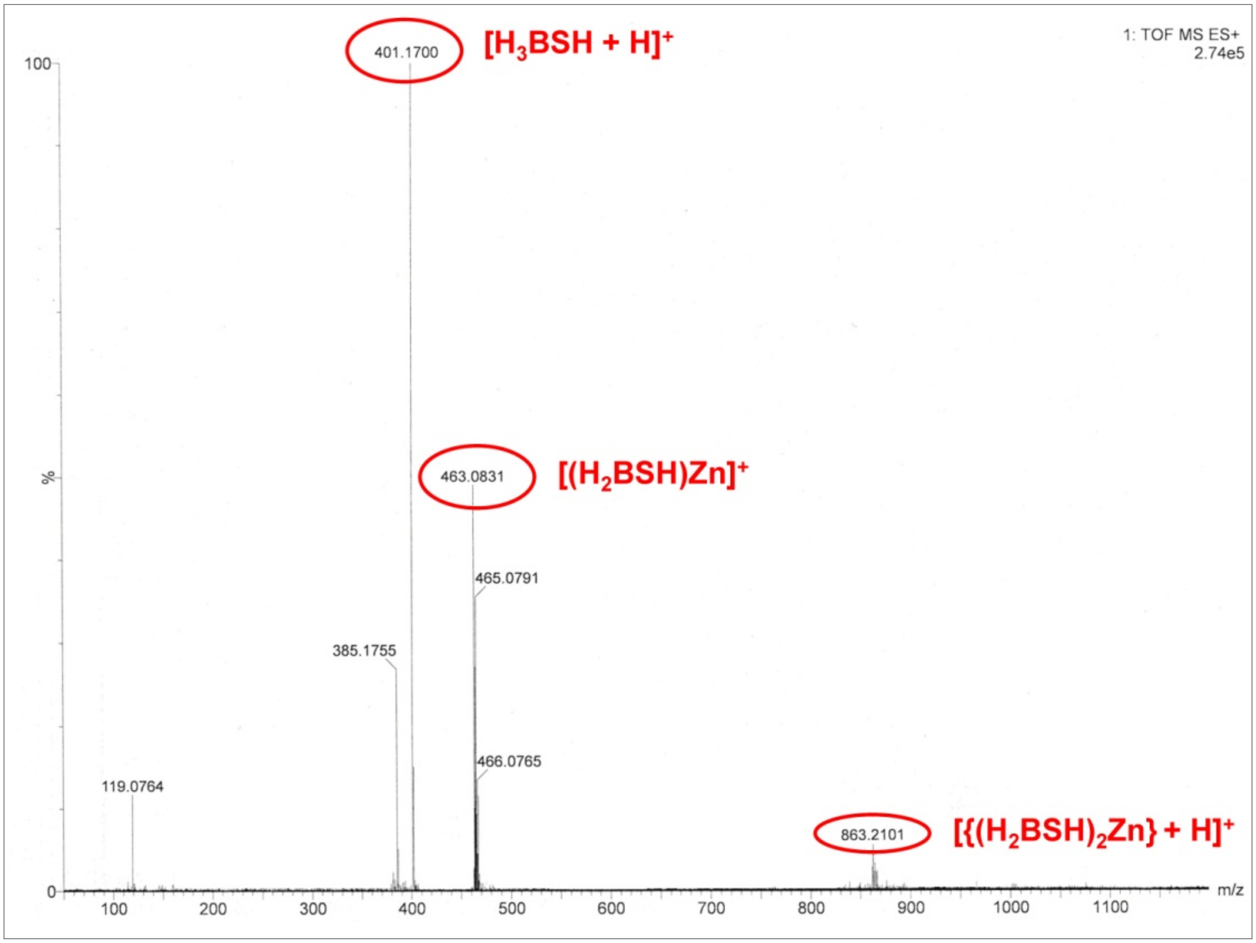

Fig. S11 ESI–MS spectrum of $[(H_2BSH)_2Zn]$ complex.

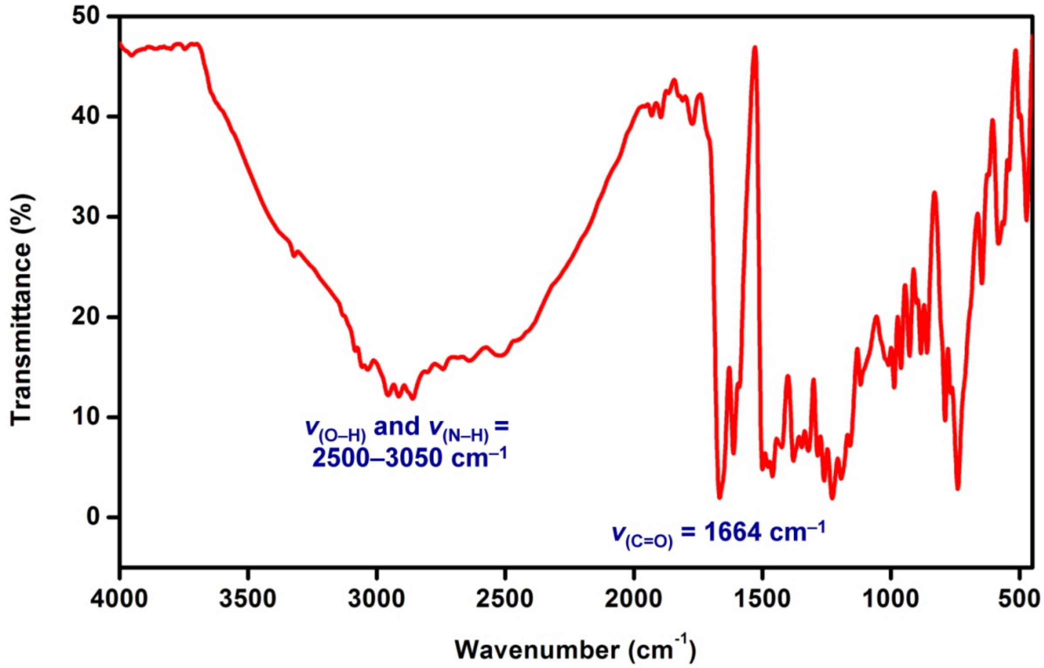

Fig. S12 FT–IR spectra of HBA.

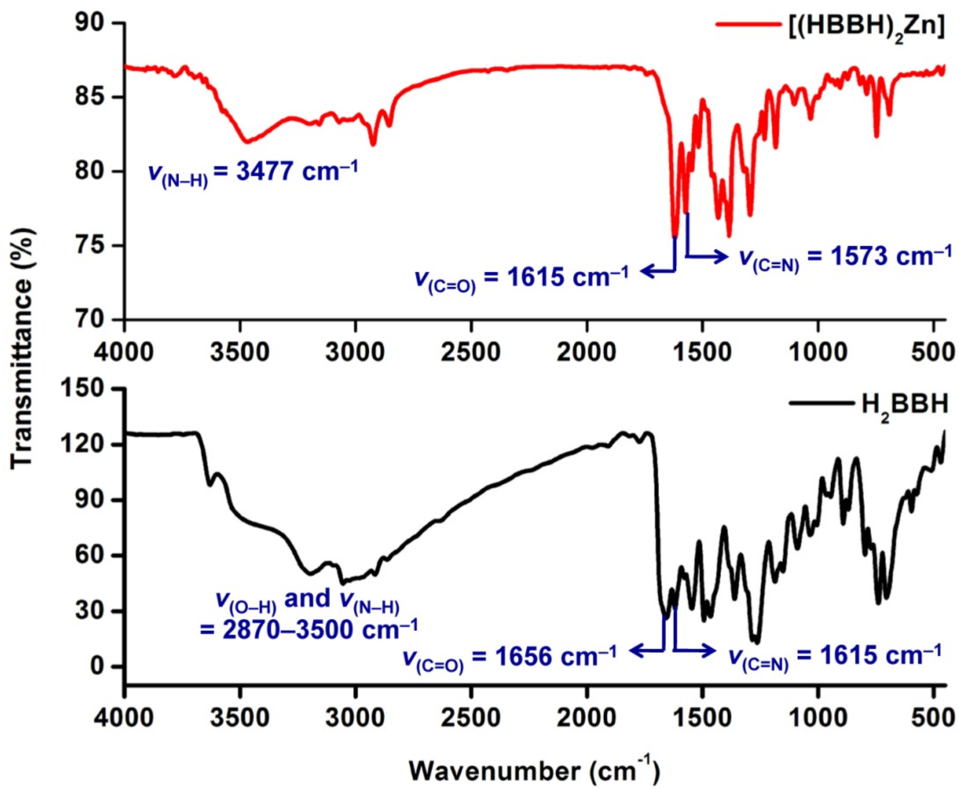

Fig. S13 FT–IR spectrum of **H_2BBH** and [(HBBH)$_2$Zn] complex.

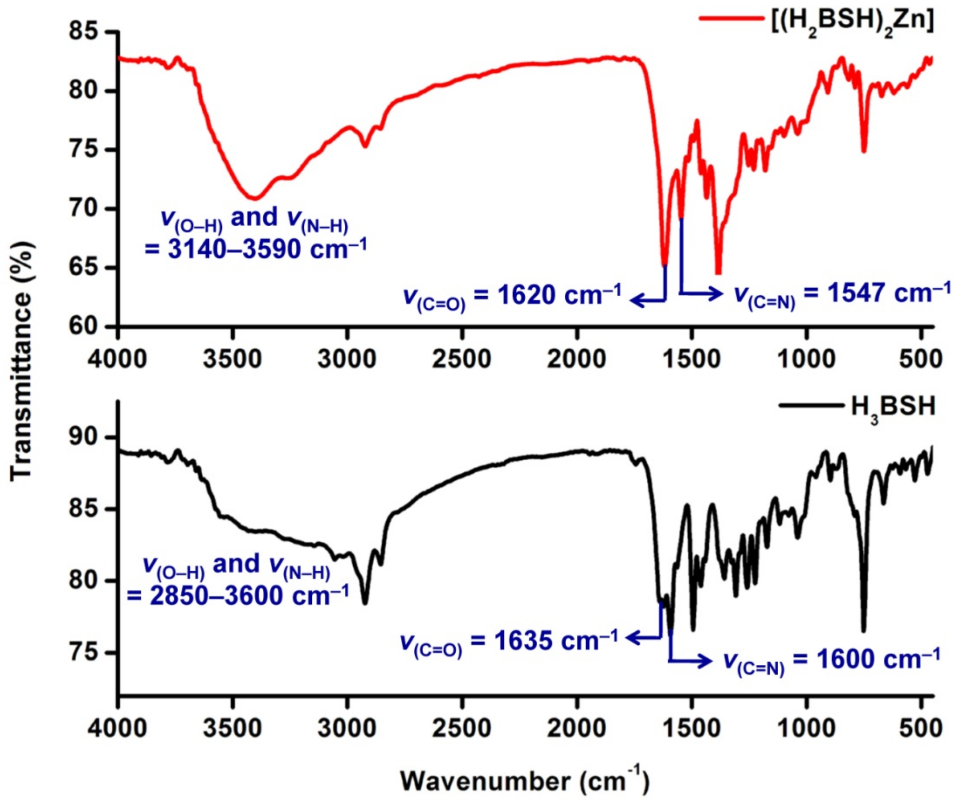

Fig. S14 FT–IR spectrum of **H_3BSH** and [$(H_2BSH)_2Zn$] complex.

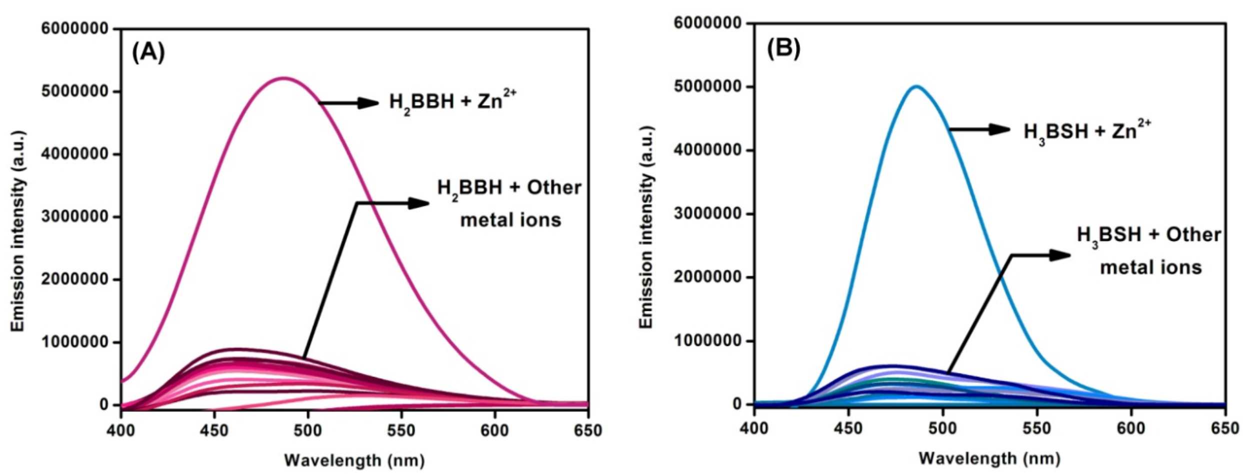

Fig. S15 Emission spectra of (A) **H_2BBH** (0.1 μM) and (B) **H_3BSH** (0.1 μM) upon addition of 1 equivalent metal ions in (1 : 1) EtOH : HEPES–buffer solution (25 mM).

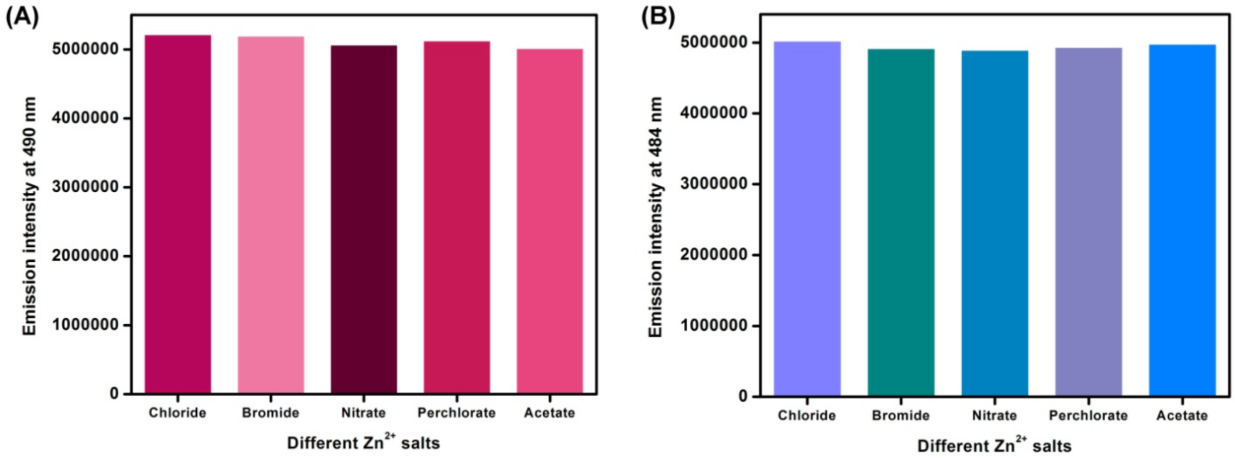

Fig. S16 Anion independent emission behavior of (A) **H_2BBH** (0.1 μM) and (B) **H_3BSH** (0.1 μM) in presence of various Zn^{2+} salts [e.g. $ZnCl_2$, $ZnBr_2$, $Zn(NO_3)_2$, $Zn(OAc)_2$ and $Zn(ClO_4)_2$ in (1 : 1) EtOH : HEPES–buffer solution (25 mM, pH = 7.2).

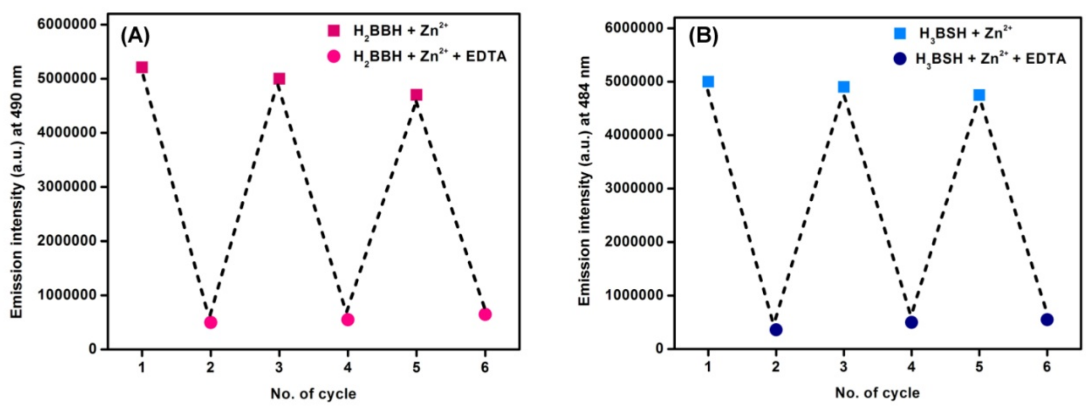

Fig. S17 Emission intensity of (A) **H_2BBH** (0.1 μM) and (B) **H_3BSH** (0.1 μM) with sequential addition of $Zn^{2+}$and EDTA in (1 : 1) EtOH : HEPES–buffer solution (25 mM).

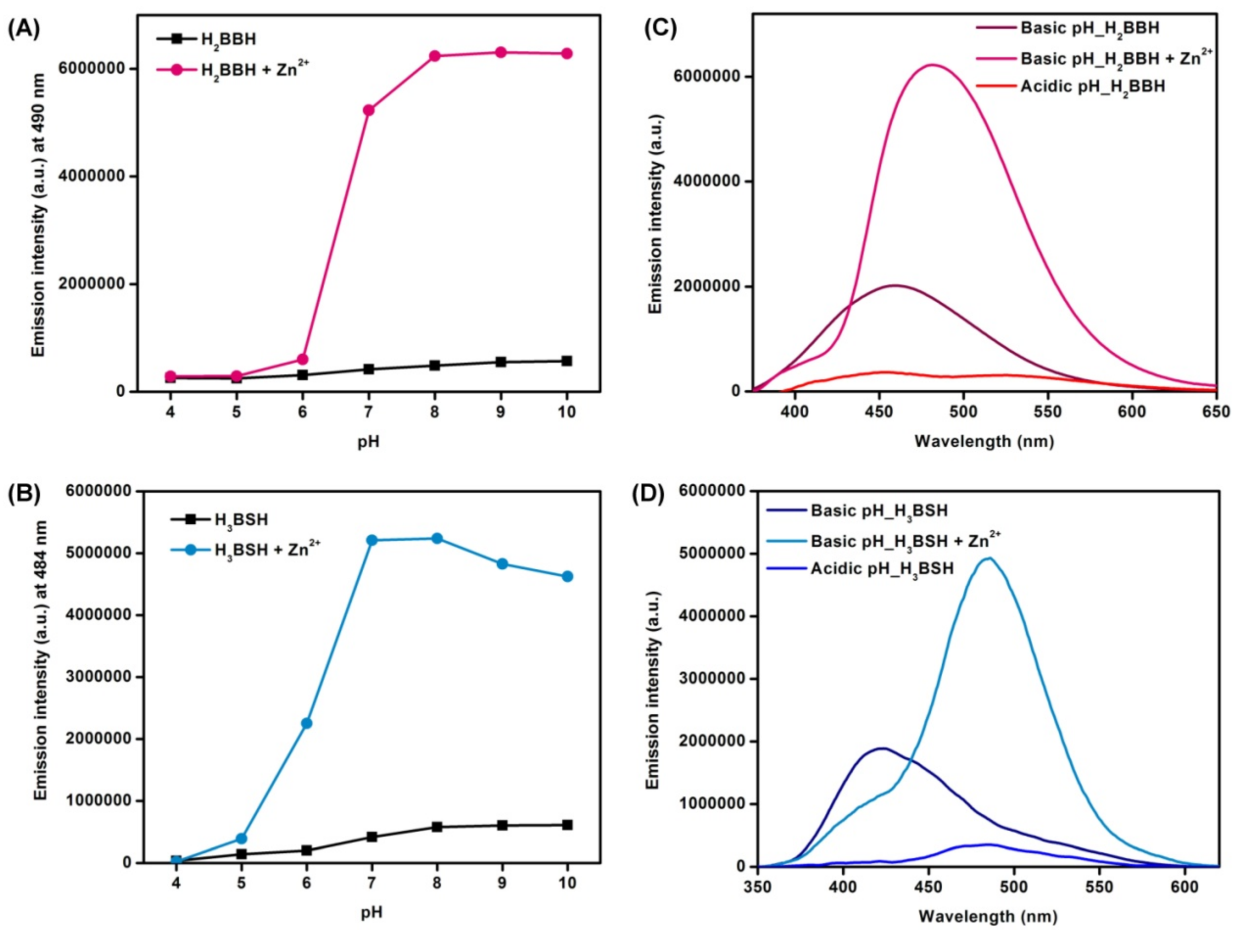

Fig. S18 Emission intensity vs pH plot of (A) **H_2BBH** (0.1 μM) (λ_{em} = 490) and (B) **H_3BSH** (0.1 μM) (λ_{em} = 484) in absence and presence of Zn^{2+} in (1 : 1) EtOH : HEPES–buffer solution (25 mM). Emission spectra of (C) **H_2BBH** (0.1 μM) and (D) **H_3BSH** (0.1 μM) in acidic and basic medium.

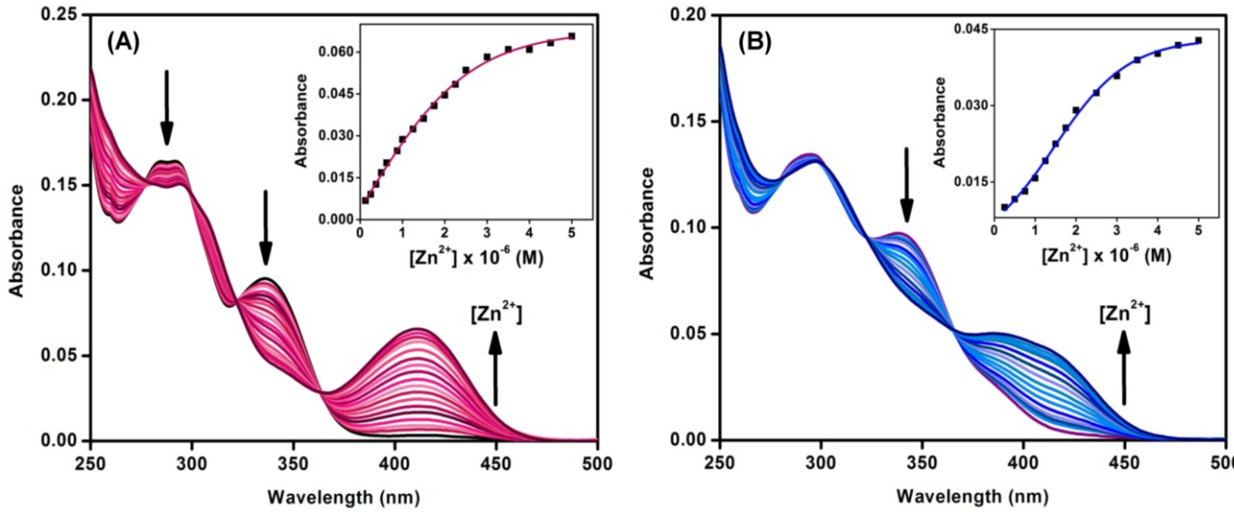

Fig. S19 UV–Vis absorption spectra of (A) **H_2BBH** (1 μM) and (B) **H_3BSH** (1 μM) upon incremental addition of Zn^{2+} in (1 : 1) EtOH : HEPES–buffer solution (25 mM). Inset: Changes in absorbance of (A) **H_2BBH** at 410 nm and (B) **H_3BSH** at 415 nm with gradual addition of Zn^{2+}.

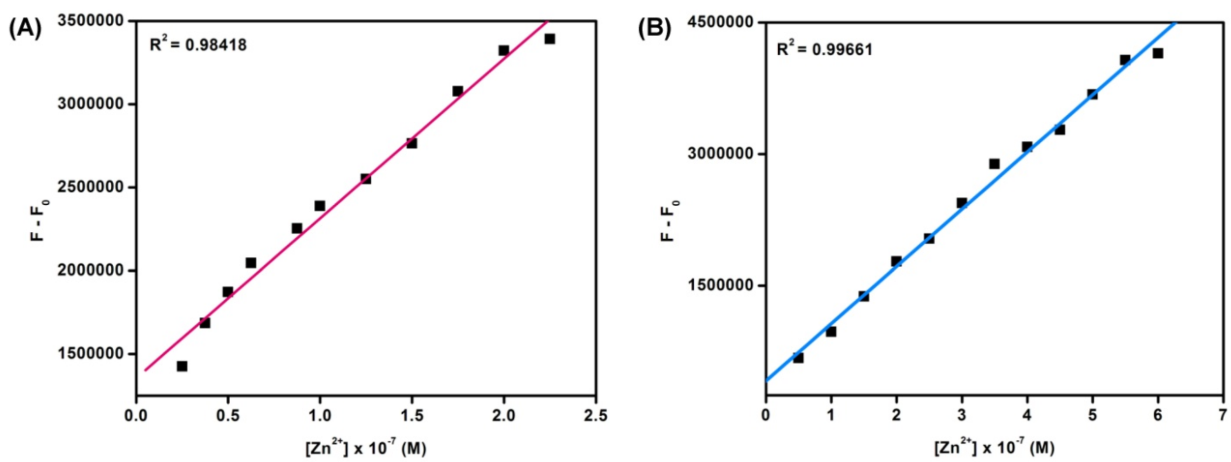

Fig. S20 Determination of the limit of detection of Zn^{2+} by (A) **H_2BBH** and (B) **H_3BSH** in (1 : 1) EtOH : HEPES–buffer solution (25 mM, pH = 7.2).

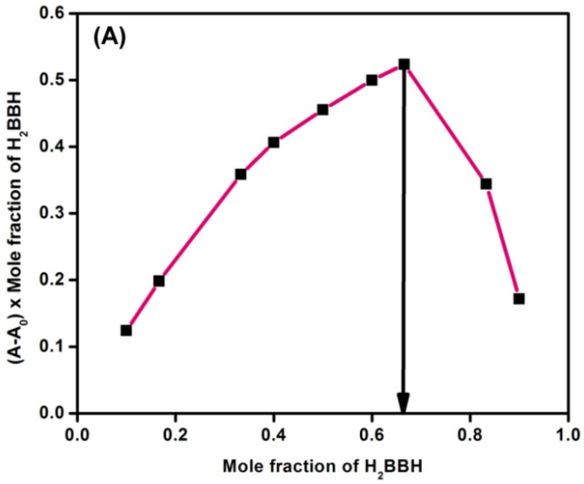

Fig. S21 Job's plot for the determination of (A) $\mathbf{H_2BBH}$–Zn^{2+} (2 : 1) and (B) $\mathbf{H_3BSH}$–Zn^{2+} (2 : 1) complex stoichiometry using absorbance values. (The Ligand ($\mathbf{H_2BBH/H_3BSH}$) : Zn^{2+} ratios used in Job's plot: 9:1, 5:1, 2:1, 3:2, 1:1, 2:3, 1:2, 1:5, and 1:9.)

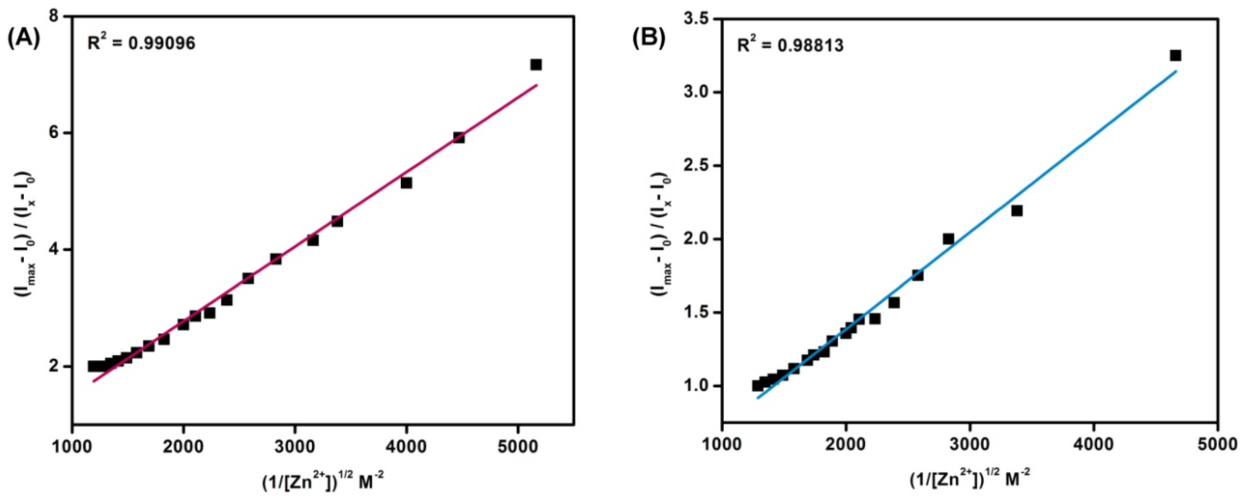

Fig. S22 Benesi−Hildebrand plot for the determination of binding constant between (A) $\mathbf{H_2BBH}$ and Zn^{2+} and (B) $\mathbf{H_3BSH}$ and Zn^{2+}.

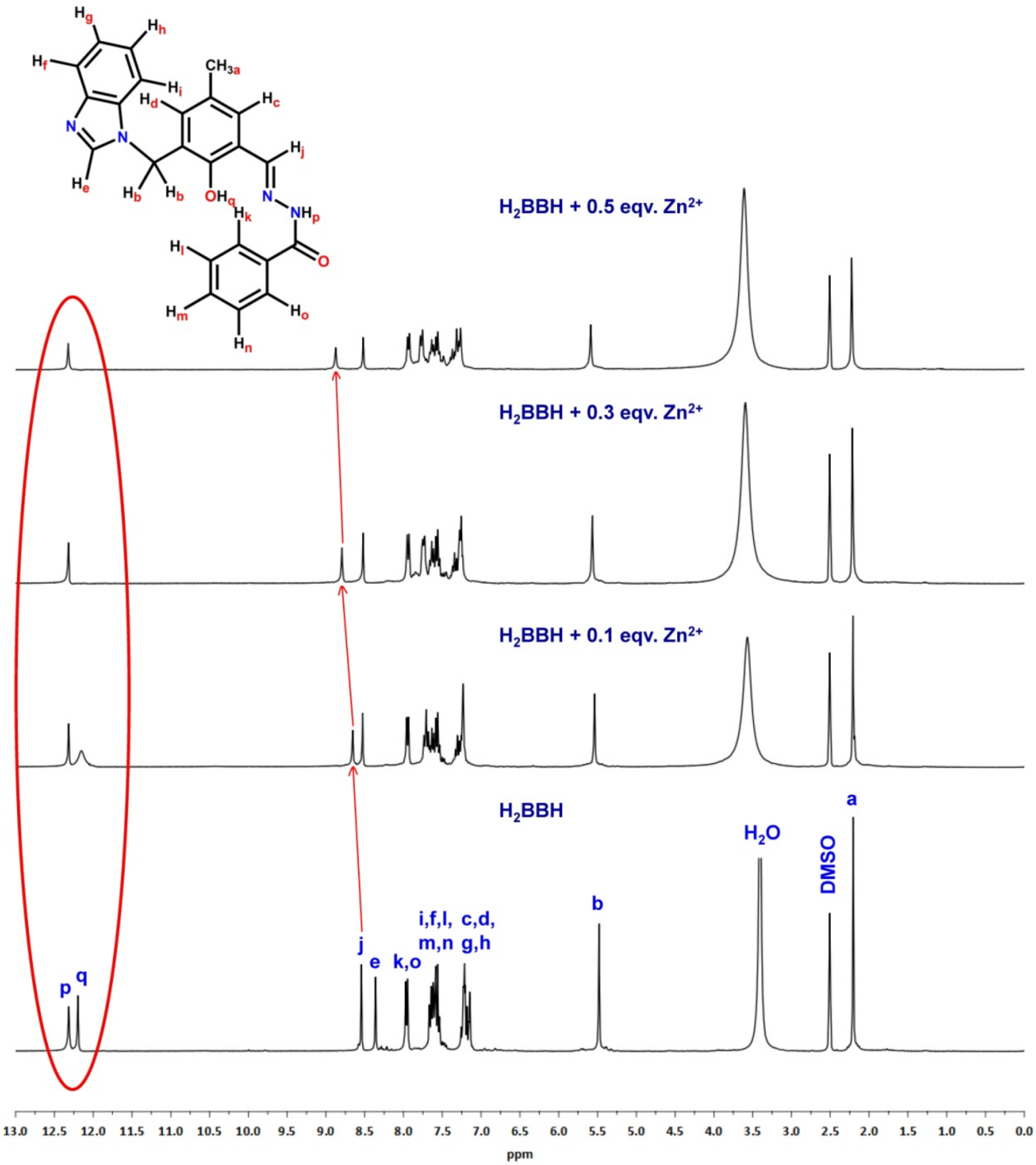

Fig. S23 ^{1}H NMR titration of **H_2BBH** in presence of Zn^{2+} in DMSO–d_6.

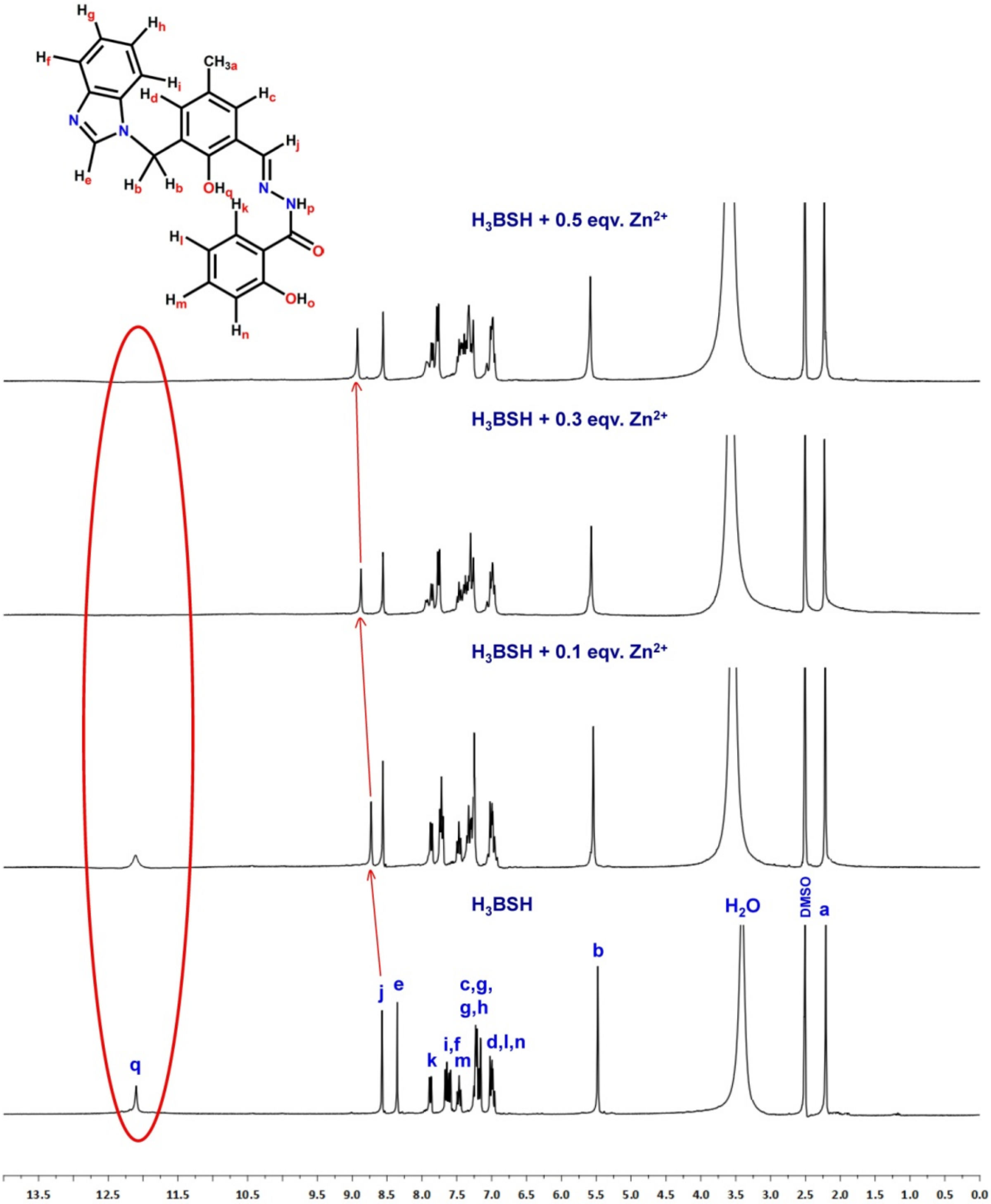

Fig. S24 ^{1}H NMR titration of **H_3BSH** in presence of Zn^{2+} in DMSO–d_6.

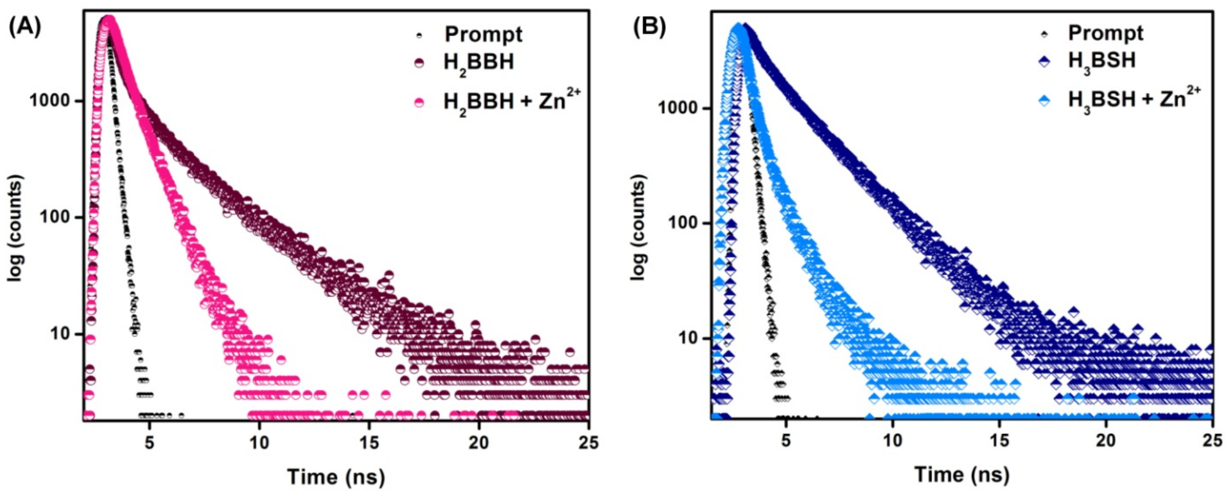

Fig. S25 Time–correlated single photon counting (TCSPC) decay profiles of (A) **H_2BBH** and **H_2BBH** + Zn^{2+} and (B) **H_3BSH** and **H_3BSH** + Zn^{2+}.

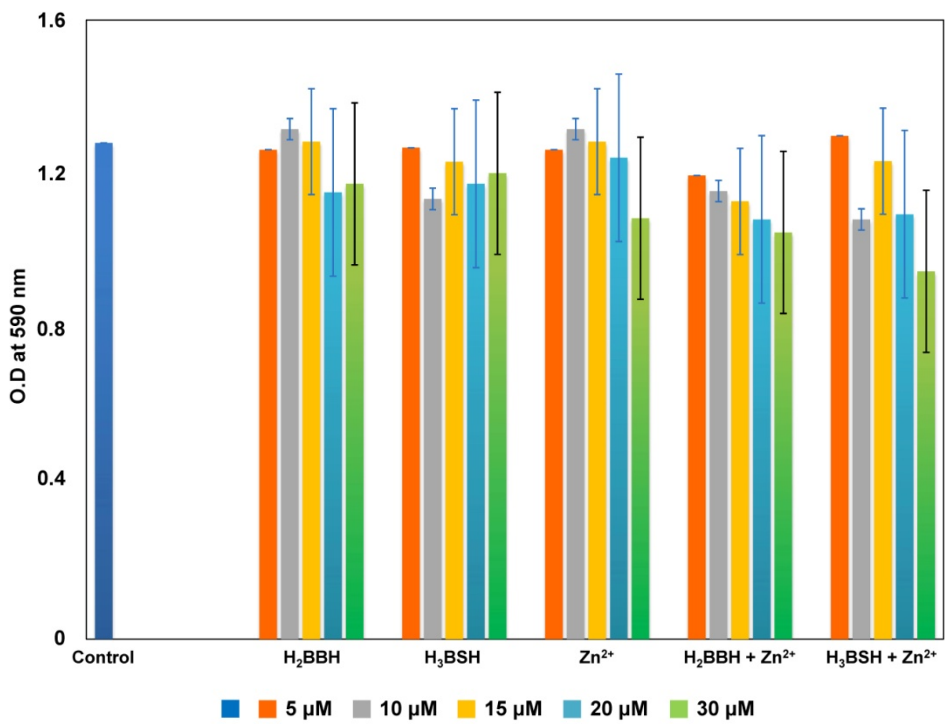

Fig. S26 MTT assay to determine the cytotoxic effect of probes, **H_2BBH** and **H_3BSH** and complexes, [(HBBH)$_2$Zn] and [(H_2BSH)$_2$Zn] on HuH–7 cells.

Table S1 List of reported acylhydrazide based dipodal Schiff base probe for detection of Zn^{2+}.

Probe	% of Water Content	Limit of Detection	λ	Reference
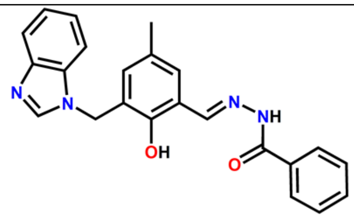	50%	27 nM	λ_{ex} = 340 nm λ_{em} = 490 nm	This work
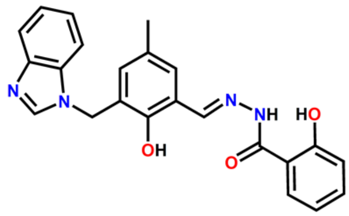		46 nM	λ_{ex} = 343 nm λ_{em} = 484 nm	
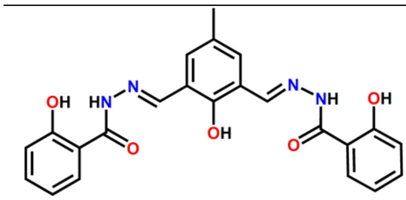	40%	44 µM	λ_{ex} = 390 nm λ_{em} = 490 nm	*Org. Biomol. Chem.*, 2012, **10**, 2380–2384
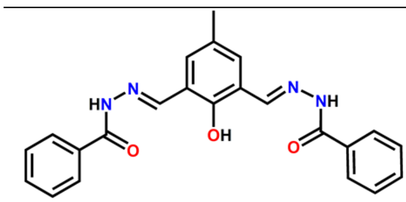	80%	0.25 µM	λ_{ex} = 370 nm λ_{em} = 497 nm	*Inorg. Chem.*, 2014, **53**, 6655–6664
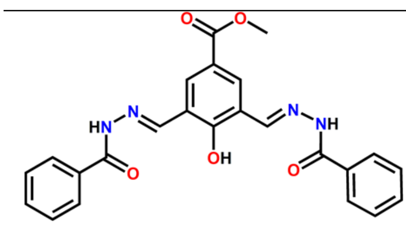	10%	0.889 µM	λ_{ex} = 407 nm λ_{em} = 457 nm	*Sens. Actuators B Chem.*, 2016, **224**, 892–898
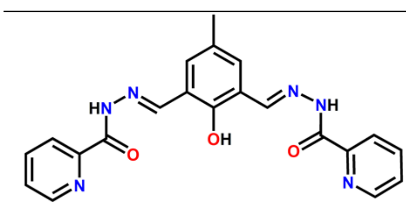	99.67%	1.05 µM	λ_{ex} = 470 nm λ_{em} = 555 nm	*Org. Biomol. Chem.*, 2014, **12**, 4975–4982
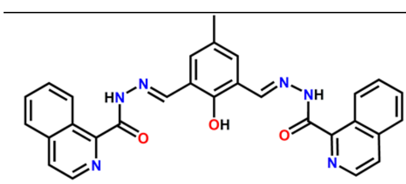	10%	0.307 µM	λ_{ex} = 460 nm λ_{em} = 536 nm	*Analyst*, 2019, **144**, 4024–4032

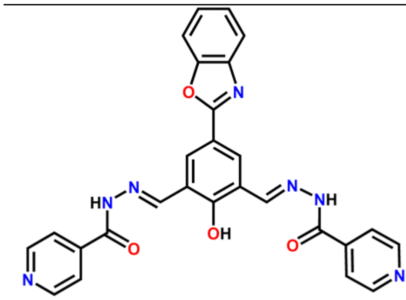	90%	0.52 μM	λ_{ex} = 450 nm λ_{em} = 525 nm	*J. Photochem. Photobio. A*, 2019, **370**, 75–83

Table S2 Tolerance limit of other metal ions.

Metal ions	Tolerance limit	
	H_2BBH	H_3BSH
Na^+	>10	>10
K^+	>10	>10
Ca^{2+}	>10	>10
Mg^{2+}	>10	>10
Al^{3+}	9	8
Cr^{3+}	7	7
Fe^{3+}	6	6
Fe^{2+}	7	6
Mn^{2+}	7	7
Co^{2+}	5	5
Ni^{2+}	4	4
Cu^{2+}	5	4
Cd^{2+}	7	7
Hg^{2+}	5	5

Table S3 ^{1}H NMR shift (ppm) data of NMR titration experiment of **H_2BBH** with Zn^{2+}.

Proton label	H_2BBH	H_2BBH + 0.1 eqv. Zn^{2+}	H_2BBH + 0.3 eqv. Zn^{2+}	H_2BBH + 0.5 eqv. Zn^{2+}
H_q	12.20	12.19	–	–
H_j	8.54	8.66	8.79	8.88

Table S4 ^{1}H NMR shift (ppm) data of NMR titration experiment of **H_3BSH** with Zn^{2+}.

Proton label	H_3BSH	H_3BSH + 0.1 eqv. Zn^{2+}	H_3BSH + 0.3 eqv. Zn^{2+}	H_3BSH + 0.5 eqv. Zn^{2+}
H_q	12.10	12.09	–	–
H_j	8.57	8.73	8.87	8.92

Table S5 Emission parameters of **H_2BBH** and **H_3BSH** in absence and presence of Zn^{2+}.

Compound	τ_1 (α_1) ns	τ_2 (α_1) ns	τ_{av} ns	χ^2	$k_r \times 10^{-2}$ ns^{-1}	$k_{nr} \times 10^{-2}$ ns^{-1}
H_2BBH	4.61 (55%)	0.46 (45%)	4.31	1.12	0.42	99.58
H_2BBH + Zn^{2+}	1.41	–	1.41	1.16	19.85	80.14
H_3BSH	4.06 (82%)	0.46 (18%)	3.97	1.15	0.35	99.64
H_3BSH + Zn^{2+}	3.98	–	3.98	1.14	6.28	93.71

Table S6 Selected MOs and TD–DFT contribution of MO towards vertical transition and corresponding oscillator strength for enol (I) and keto (II) conformers of **H_2BBH**.

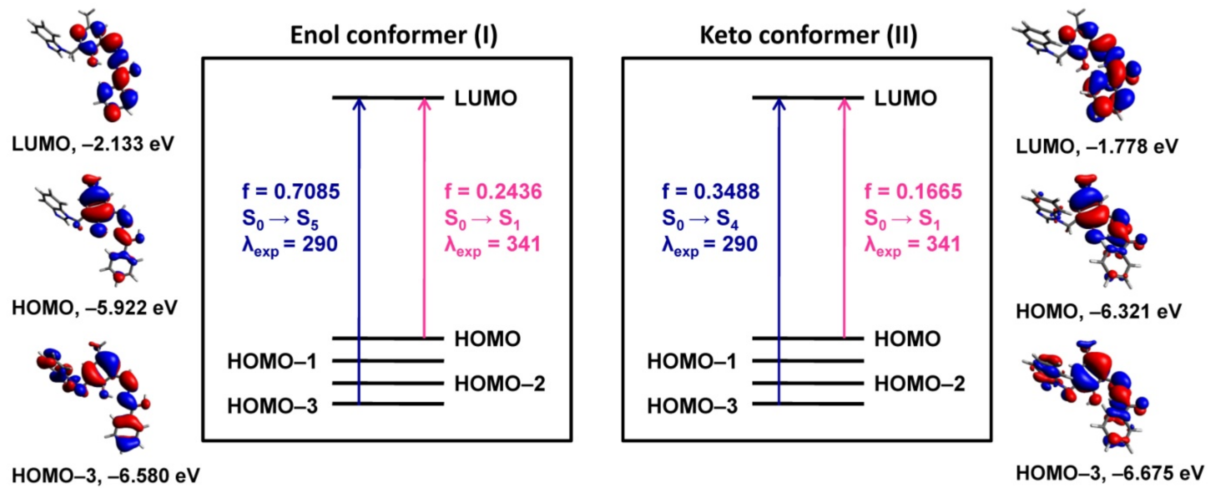

Electronic transitions	**Composition**	**Excitation energy (λ)**	**Oscillator strength (*f*)**	**λ_{exp} (nm)**
		Enol conformer (I)		
$S_0 \rightarrow S_1$	HOMO → LUMO (93%)	3.138 eV (395 nm)	0.2436	341
$S_0 \rightarrow S_5$	HOMO–3 → LUMO (89%)	4.057 eV (305 nm)	0.7085	290
		Keto conformer (II)		
$S_0 \rightarrow S_1$	HOMO → LUMO (92%)	3.798 eV (326 nm)	0.1665	341
$S_0 \rightarrow S_4$	HOMO–3 → LUMO (85%)	4.336 eV (286 nm)	0.3488	290

Table S7 Selected MOs and TD–DFT contribution of MO towards vertical transition and corresponding oscillator strength for enol (I) and keto (II) conformers of $\mathbf{H_3BSH}$.

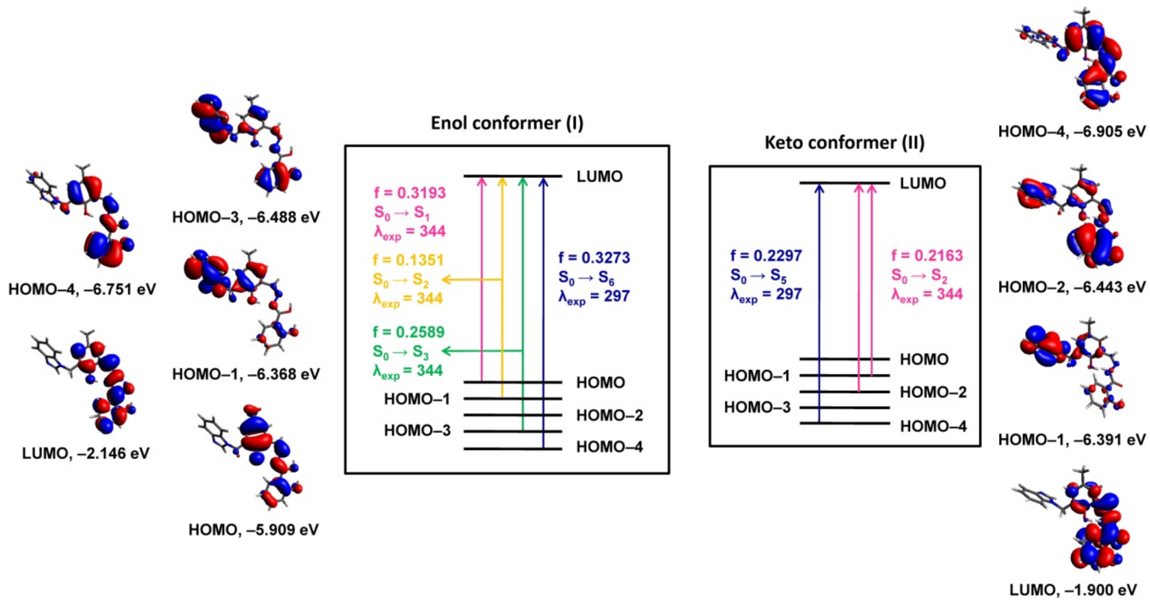

Electronic transitions	**Composition**	**Excitation energy (λ)**	**Oscillator strength (*f*)**	**λ_{exp} (nm)**
		Enol conformer (I)		
$S_0 \rightarrow S_1$	HOMO → LUMO (93%)	3.181 eV (390 nm)	0.3193	
$S_0 \rightarrow S_2$	HOMO–1 → LUMO (96%)	3.253 eV (381 nm)	0.1351	344
$S_0 \rightarrow S_3$	HOMO–3 → LUMO (83%)	3.708 eV (334 nm)	0.2589	
$S_0 \rightarrow S_6$	HOMO–4 → LUMO (83%)	4.175 eV (297 nm)	0.3273	297
		Keto conformer (II)		
$S_0 \rightarrow S_2$	HOMO–2 → LUMO (66%) HOMO–1 → LUMO (23%)	3.922 eV (316 nm)	0.2163	344
$S_0 \rightarrow S_5$	HOMO–4 → LUMO (94%)	4.377 eV (283 nm)	0.2297	297

Table S8 Selected MOs and TD–DFT contribution of MO towards vertical transition and corresponding oscillator strength for $[(HBBH)_2Zn]$ complex.

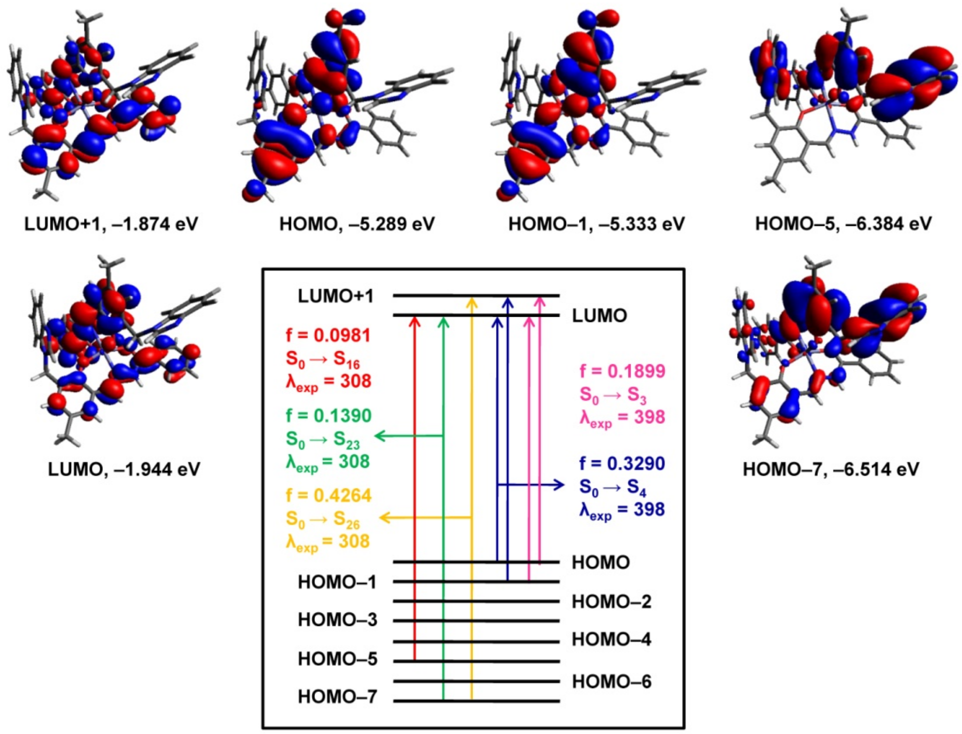

Electronic transitions	Composition	Excitation energy (λ)	Oscillator strength (*f*)	λ_{exp} (nm)
$S_0 \rightarrow S_3$	HOMO–1 → LUMO (34%) HOMO → LUMO+1 (56%)	2.863 eV (433 nm)	0.1899	410
$S_0 \rightarrow S_4$	HOMO–1 → LUMO+1 (67%) HOMO → LUMO (18%)	2.926 eV (423 nm)	0.3290	
$S_0 \rightarrow S_{16}$	HOMO–5 → LUMO (55%)	3.800 eV (326 nm)	0.0981	296
$S_0 \rightarrow S_{23}$	HOMO–7 → LUMO (80%)	3.970 eV (312 nm)	0.1390	
$S_0 \rightarrow S_{26}$	HOMO–7 → LUMO+1 (71%)	4.170 eV (297 nm)	0.4264	

Table S9 Selected MOs and TD–DFT contribution of MO towards vertical transition and corresponding oscillator strength for $[(H_2BSH)_2Zn]$ complex.

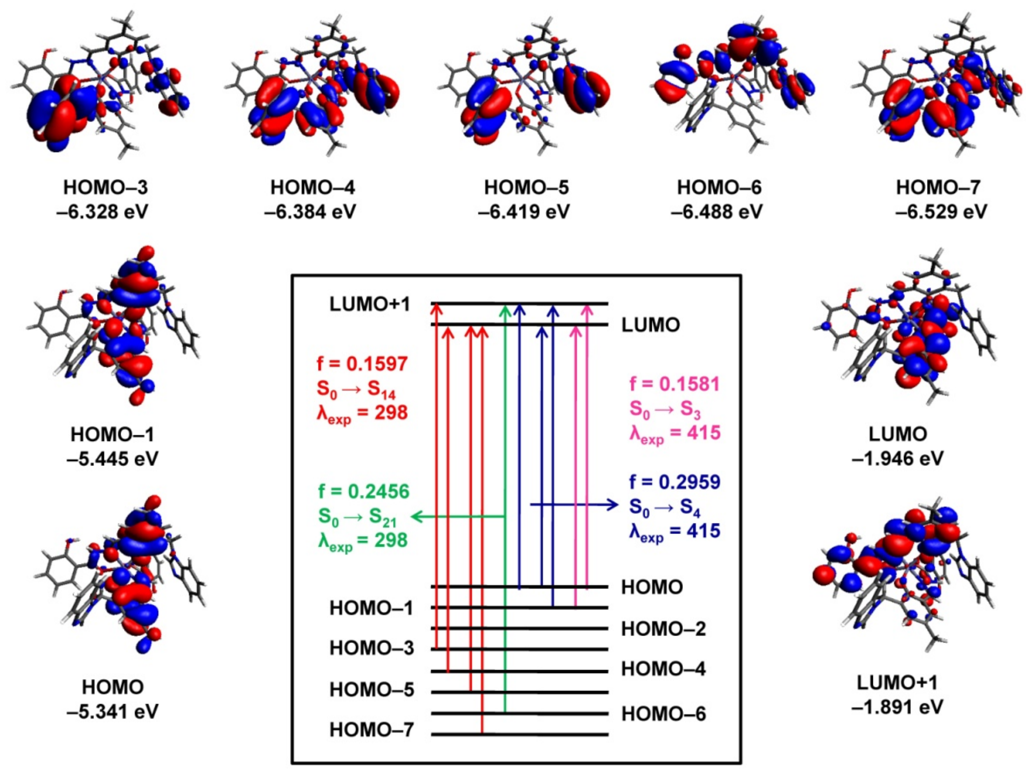

Electronic transitions	Composition	Excitation energy (λ)	Oscillator strength (*f*)	λ_{exp} (nm)
$S_0 \rightarrow S_3$	HOMO–1 → LUMO (64%) HOMO → LUMO+1 (21%)	2.897 eV (428 nm)	0.1581	415
$S_0 \rightarrow S_4$	HOMO–1 → LUMO+1 (69%) HOMO → LUMO (10%) HOMO → LUMO+1 (10%)	3.021 eV (410 nm)	0.2959	
$S_0 \rightarrow S_{14}$	HOMO–7 → LUMO (20%) HOMO–5 → LUMO (13%) HOMO–4 → LUMO (15%) HOMO–3 → LUMO+1 (28%)	3.863 eV (320 nm)	0.1597	298
$S_0 \rightarrow S_{21}$	HOMO–6 → LUMO+1 (68%)	4.110 eV (301 nm)	0.2456	